Phytic acid-derivative Co$_2$B-CoPO$_x$ coralloidal structure with delicate boron vacancy for enhanced hydrogen generation from sodium borohydride

Luyan Shi [a], Ke Zhu [a], Yuting Yang [a], Qinrui Liang [a], Qimin Peng [a], Shuqing Zhou [a], Tayirjan Taylor Isimjan [b,*], Xiulin Yang [a,*]

[a] Guangxi Key Laboratory of Low Carbon Energy Materials, School of Chemistry and Pharmaceutical Sciences, Guangxi Normal University, Guilin 541004, China
[b] Saudi Arabia Basic Industries Corporation (SABIC) at King Abdullah University of Science and Technology (KAUST), Thuwal 23955-6900, Saudi Arabia

A B S T R A C T

Application of transition metal boride (TMB) catalysts towards hydrolysis of NaBH$_4$ holds great significance to help relieve the energy crisis. Herein, we present a facile and versatile metal-organic framework (MOF) assisted strategy to prepare Co$_2$B-CoPO$_x$ with massive boron vacancies by introducing phytic acid (PA) cross-linked Co complexes that are acquired from reaction of PA and ZIF-67 into cobalt boride. The PA etching effectively breaks down the structure of ZIF-67 to create more vacancies, favoring the maximal exposure of active sites and elevation of catalytic activity. Experimental results demonstrate a drastic electronic interaction between Co and the dopant phosphorous (P), thereby the robustly electronegative P induces electron redistribution around the metal species, which facilitates the dissociation of B-H bond and the adsorption of H$_2$O molecules. The vacancy-rich Co$_2$B-CoPO$_x$ catalyst exhibits scalable performance, characterized by a high hydrogen generation rate (HGR) of 7716.7 mL min^{-1} g^{-1} and a low activation energy (E_a) of 44.9 kJ/mol, rivaling state-of-the-art catalysts. This work provides valuable insights for the development of advanced catalysts through P doping and boron vacancy engineering and the design of efficient and sustainable energy conversion systems.

Hydrogen-related energy devices, including hydrogen-oxygen fuel cells, large-scale hydrogen power generation, and other hydrogen-powered devices, have incentivized the revolution of various hydrogen evolution technologies [1]. In particular, hydrogen storage materials catalytic hydrogen (H$_2$) generation technology has been deemed an up-and-coming trend to realize a sustainable energy scheme [2]. Among the chemical storage sources of hydrogen, metal hydrides such as NaBH$_4$, LiAlH$_4$ and MgH$_2$ have garnered tremendous recent attention [3–5]. Among them, NaBH$_4$ is emerging as a central focus with a theoretical gravimetric hydrogen storage capacity of 10.6 wt%, excellent hydrolysis

atoms [14,15]. In addition, high electronegative heteroatom doping can increase the number and modulate the electronic surrounding of metal active sites, thus improving the activities of the catalyst [16]. For example, Mehdi *et al.* reported P-induced Co-based monolithic efficient catalysts for NH_3BH_3 hydrolysis and showed that the induction of P caused electron transfer from Co to P, promoting new active sites for the efficient adsorption of reactant molecules [17]. Notably, the highly electronegative phosphorus (P) atom possesses lone-pair electrons in 3p orbitals and vacant 3d orbitals, which can mediate local charge density and change the surface charge state, further advancing the catalytic performance [18]. We assume that the P-induced approach also has a positive effect on the catalyst of $NaBH_4$ hydrolysis. However, conventional procedures (gas-solid reaction scheme) use NaH_2PO_2 as the P source, which would release poisonous and auto-ignition PH_3 products into the environment [19]. Phytic acid (PA, myo-inositol 1,2,3,4,5,6-hexakisphosphate) is a naturally environmentally friendly and renewable biological compound, and its six phosphate groups can easily chelate to different metal ions, which can serve as an ideal P source to replace NaH_2PO_2 [20]. In the processes of PA etching, P possesses higher electronegativity than metallic (M) atoms, which tend to receive electrons from the metal, causing a redistribution of the electronic properties of the catalysts and further forming the key active sites favoring the interaction and adsorption with reaction intermediates [21]. On the other hand, vacancy engineering is considered a new "intrinsic" strategy to enhance catalytic activity by inducing high distortion energy and diverse atomic rearrangements [22]. Besides, vacancies can manipulate the electronic band structure as well as lower the activation energy of adsorption and dissociation of reactants [23]. Consequently, the electronic structure and surface nature of the catalyst are two versatile knobs for enhancing the intrinsic catalytic activity, which can be favorably tailored through doping and vacancy engineering.

In this work, a light P doping and rich boron vacancies Co_2B-$CoPO_x$ was developed as a highly efficient catalyst for $NaBH_4$ hydrolysis. The coralloidal structure of Co_2B-$CoPO_x$ is porous with an average pore size of about 23.8 nm. Such unique structural features not only provide more active sites but also may improve electron transfer dynamics, beneficial to the hydrolysis of $NaBH_4$. Moreover, the experimental and characteristic analyses show that the doping of P tunes the relative content of B and induces more boron vacancies, which subsequently affects the electronic structure and facilitates the reversible dissociation of B-H on active sites. As a result, Co_2B-$CoPO_x$ exhibits excellent hydrolysis activity and scalable reusability. Importantly, the prepared robust Co_2B-$CoPO_x$ catalyst reveals remarkably efficient hydrogen evolution from $NaBH_4$ in comparison to previous non-noble catalysts and even noble catalysts presented in the literature. Our work provides new opportunities for designing advanced metal borides catalysts for the hydrolysis of
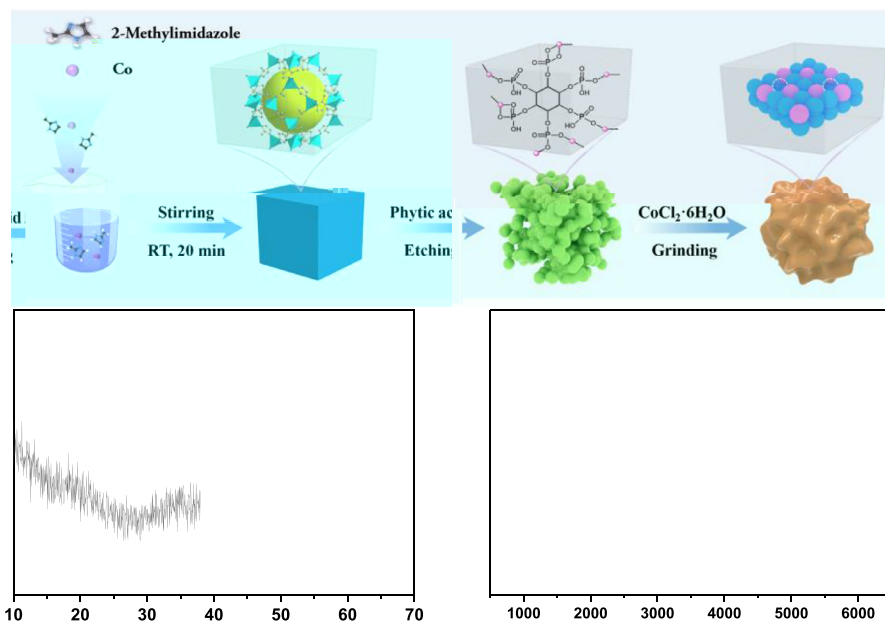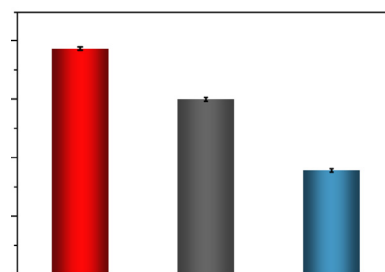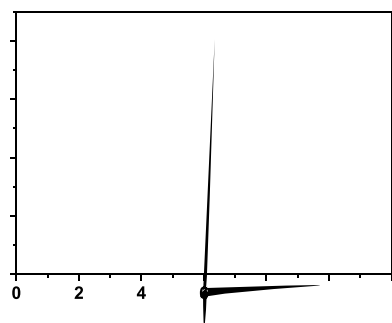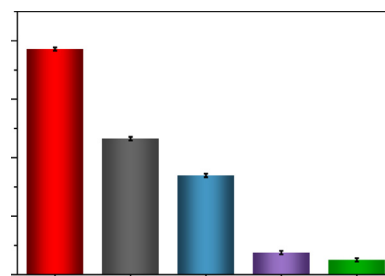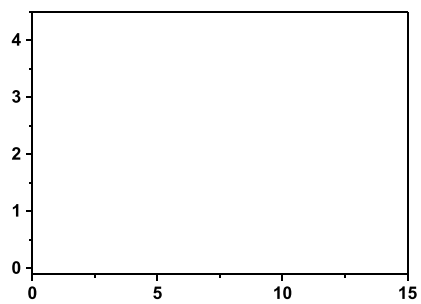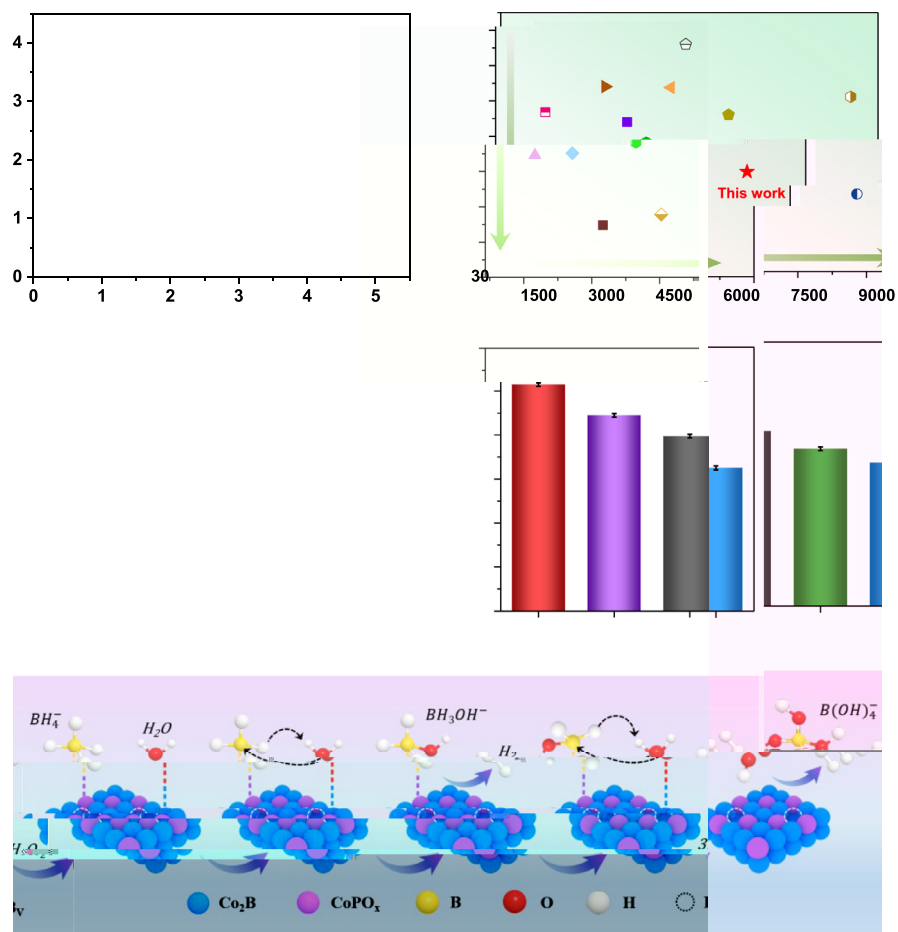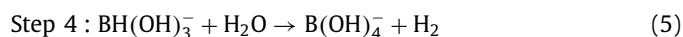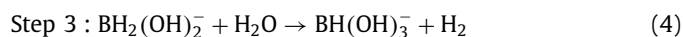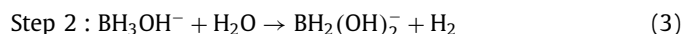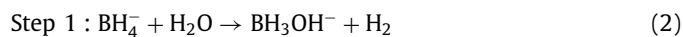
hydrolysis process [59]. The amount of catalyst is another decisive factor in determining the catalytic reaction rate. As seen in Figs. S15c and d (Supporting information), the hydrogen generation rate of Co_2B-$CoPO_x$ varied with the change in catalyst mass from 5 mg to 20 mg. Among the series, 10 mg of Co_2B-$CoPO_x$ exhibited the highest hydrogen generation rate, making it the optimal amount of catalyst and resulting in substantial cost reduction.

The effect of P doping on the activation energy in $NaBH_4$ hydrolysis was explored by investigating the temperature dependence of hydrogen generation kinetics at different temperatures, as shown in Fig. 4a and Fig. S16a (Supporting information). Based on the Arrhenius plots, the activation energy (E_a) value of Co_2B-$CoPO_x$ was calculated to be 44.9 kJ/mol, which is lower than that of Co_2B-ZIF-67 (56.1 kJ/mol) (Fig. S16b in Supporting information), and significantly lower than the values reported for most non-noble or noble mental catalysts in previous literature (Fig. 4b). This validates that P doping effectively reduced the energy barrier for molecule activation. Hydrogen generation with NH_3BH_3 is proceeded under a similar method. A HGR of 1891.9 mL min^{-1} g^{-1} is achieved (Fig. S17 in Supporting information). Compared with $NaBH_4$ (7716.7 mL min^{-1} g^{-1}), a decreased activity is emerged for NH_3BH_3 hydrolysis. This negative activity is attributed to the discrepant catalytic mechanism during borohydride hydrolysis caused by the different molecular geometry of $NaBH_4$ and NH_3BH_3 [60]. The reusability is very important for catalysts in the aspect of the practical application. Therefore, the reusability of Co_2B-$CoPO_x$ catalyst was evaluated through a continuous recycling test of catalytic $NaBH_4$ hydrolysis. As depicted in Figs. 4c and d, the catalyst exhibited a slight degradation in activity after 5 cycles. As demonstrated in Fig. S18 (Supporting information), the XRD pattern shows that the Co_2B-$CoPO_x$ after 5 cycles keeps a similar structural composition. Moreover, XPS analysis (Fig. S19 in Supporting information) exhibits that the original elemental composition, chemical state and the peak intensities were similar to Co_2B-$CoPO_x$ even after 5 cycles. These results clearly indicate that our developed catalyst bears a stable coralloidal structure. The SEM images show that the catalyst's surface occurs agglomerations after catalyzing the hydrolysis of $NaBH_4$ (Fig. S20 in Supporting information). Therefore, the slight decrease in catalytic activity can be attributed to surface agglomeration and accumulation of metaborate on the catalyst surface, resulting in a reduction of boron vacancies and thus hindering electron transmission [61,62]. Overall, the Co_2B-$CoPO_x$ catalyst demonstrated outstanding activity and reusability, making it cost-effective and suitable for practical industrial applications.

We next tried to shed light on the underlying origin of the striking catalysis performance of Co_2B-$CoPO_x$ based on Langmuir-Hinshelwood model and many previous literatures, the plausible mechanism for $NaBH_4$ hydrolysis over Co_2B-$CoPO_x$ catalyst is shown in Eqs. 2–5 and Fig. 4e [55,61,63]. According to XPS study, P species, being strongly electronegative, draw electrons from Co_2B, resulting in a higher electron density on $CoPO_x$ species compared to Co_2B species. Consequently, the B atoms with a few positive charges in BH_4^- ions are adsorbed by the electron-rich $CoPO_x$ species through the binding sites provided by boron vacancies, while the electron-deficient Co_2B species adsorb H_2O molecules. In step 1, the adsorbed water molecule attacks BH_4^-. Consequently, one molecule of H_2 is released and an adsorbed BH_3OH^- is lefts on the surface. In step 2, another adsorbed H_2O molecule attacks BH_3OH^-, and the second H_2 molecule is released and the $BH_2(OH)_2^-$ is produced and lefts on the $CoPO_x$ species surface. In step 3, a new H_2O molecule adsorbs at Co_2B species and attacks $BH_2(OH)_2^-$ to produce $BH(OH)_3^-$ and H_2. In step 4, H_2O molecule attacks $BH(OH)_3^-$ to give H_2 and $B(OH)_4^-$. Meanwhile, the $B(OH)_4^-$ is desorbs. Therefore, the hydrolysis reaction ends with compete conversion of BH_4^- ion to $B(OH)_4^-$ ion with release of four H_2 molecules [64]. This mechanism highlights the role

of P doping and B vacancy engineering in the Co_2B-$CoPO_x$ catalyst, where P enhances the electron density of $CoPO_x$ species, facilitating the adsorption of B atoms through boron vacancies. This unique interaction between the catalyst and reactants promotes the efficient hydrolysis of $NaBH_4$, leading to enhanced catalytic activity and hydrogen generation.

$$\text{Step 1}: BH_4^- + H_2O \rightarrow BH_3OH^- + H_2 \tag{2}$$

$$\text{Step 2}: BH_3OH^- + H_2O \rightarrow BH_2(OH)_2^- + H_2 \tag{3}$$

$$\text{Step 3}: BH_2(OH)_2^- + H_2O \rightarrow BH(OH)_3^- + H_2 \tag{4}$$

$$\text{Step 4}: BH(OH)_3^- + H_2O \rightarrow B(OH)_4^- + H_2 \tag{5}$$

In conclusion, we report that the P doping rich boron vacancy on Co_2B-$CoPO_x$ can be achieved through chelating Co with negatively charged phosphate groups. The rational P doping strategy simultaneously realized the high-level chemical induction and defects in the catalyst. The presence of abundant boron vacancy enhances the catalyst's capacity to capture and interact with reaction intermediates effectively. The high electronegativity of P species serves as an electronic structure modifier to tune the local charge of Co *via* electron transfer, creating favorable condition for the dissociation of B-H and O−H bonds and rendering impressive catalytic activity. The hydrolysis of $NaBH_4$ measurements certify the exceptional activity of Co_2B-$CoPO_x$, with a hydrogen generation rate (HGR) of 7716.7 mL min^{-1} g^{-1}, which is 2.3 times higher than that of Co_2B-ZIF-67. Furthermore, Co_2B-$CoPO_x$ exhibited superior reusability, making it highly promising for practical large-scale applications. These findings provide important design guidance for various hydrogen-involving applications, offering new opportunities for the development of efficient and sustainable energy systems.

Declaration of competing interest

The authors declare that they have no known competing financial interests or personal relationships that could have appeared to influence the work reported in this paper.

Acknowledgments

Supplementary materials

Supplementary material associated with this article can be found, in the online version, at doi:10.1016/j.cclet.2023.109222.

References

[1] M. Li, Z. Zhao, Z. Xia, et al., Angew. Chem. Int. Ed. 60 (2021) 8243–8250.
[2] Z. Gao, G. Wang, T. Lei, et al., Nat. Commun. 13 (2022) 118.
[3] S.S. Liu, Z.B. Li, C.L. Jiao, et al., Int. J. Hydrog. Energy 38 (2013) 2770–2777.
[4] C. Saka, Appl. Catal. B: Environ. 292 (2021) 120165.
[5] Q. Yao, X. Zhang, Z.H. Lu, Q. Xu, Coord. Chem. Rev. 493 (2023) 215302.
[6] L. Ouyang, W. Chen, J. Liu, et al., Adv. Energy Mater. 7 (2017) 1700299.
[7] L. Yao, X. Li, W. Peng, et al., Inorg. Chem. Front. 8 (2021) 1056–1065.
[8] Y. Zhu, L. Ouyang, H. Zhong, et al., Angew. Chem. Int. Ed. 59 (2020) 8623–8629.
[9] H.X. Nunes, D.L. Silva, C.M. Rangel, A.M.F.R. Pinto, Energies 14 (2021) 3567.
[10] A.F. Baye, M.W. Abebe, R. Appiah-Ntiamoah, H. Kim, J. Colloid Interface Sci. 543 (2019) 273–284.

[11] H. Zhang, G. Xu, L. Zhang, et al., Renew. Energy 162 (2020) 345–354.
[12] X. Zhang, X. Sun, D. Xu, et al., Appl. Surf. Sci. 469 (2019) 764–769.
[13] C. Wu, J. Guo, J. Zhang, et al., Renew. Energy 136 (2019) 1064–1070.
[14] X. Wang, J. Liao, H. Li, H. Wang, R. Wang, Int. J. Hydrog. Energy 42 (2017) 6646–6656.
[15] Z. Liu, Y. Tian, S. Li, et al., Adv. Funct. Mater. 33 (2023) 2301994.
[16] H. Sun, J. Meng, L. Jiao, F. Cheng, J. Chen, Inorg. Chem. Front. 5 (2018) 760–772.
[17] S. Mehdi, Y. Liu, H. Wei, et al., Appl. Catal. B: Environ. 325 (2023) 122317.
[18] Z. Xiao, Y. Wang, Y.C. Huang, et al., Energy Environ. Sci. 10 (2017) 2563–2569.
[19] Y. Fan, Y. Zhou, L. Zhang, Y. Feng, K. Shih, Sep. Purif. Technol. 264 (2021) 118367.
[20] G. Zhang, G. Wang, Y. Liu, et al., J. Am. Chem. Soc. 138 (2016) 14686–14693.
[21] J. Zhang, J. Zhang, F. He, et al., Nano Micro Lett. 13 (2021) 65.
[22] X. Wang, Y. Zhang, H. Si, et al., J. Am. Chem. Soc. 142 (2020) 4298–4308.
[23] W. Zhong, Z. Wang, N. Gao, et al., Angew. Chem. Int. Ed. 59 (2020) 22743–22748.
[24] Y. Shan, M. Zhang, Y. Bai, et al., Chem. Eng. J. 429 (2022) 132146.
[25] L. He, Y. Cheng, Q. Li, et al., Chem. Eng. J. 453 (2023) 139566.
[26] S. Sun, Y. Tang, C. Wu, C. Wan, Anal. Chim. Acta 1107 (2020) 55–62.
[27] X. Wang, Z. Na, D. Yin, et al., ACS Nano 12 (2018) 12238–12246.
[28] T. Chen, F. Wang, S. Cao, et al., Adv. Mater. 34 (2022) 2201779.
[29] W. Peng, S. Liu, X. Li, et al., Chin. Chem. Lett. 33 (2022) 1403–1406.
[30] C. Yan, Q. Ma, F. Wang, et al., Chem. Eng. J. 433 (2022) 133651.
[31] P. Wu, Q. Jia, J. He, et al., J. Hazard. Mater. 391 (2020) 122183.
[32] J. Xiong, J. Luo, L. Yang, et al., J. Ind. Eng. Chem. 64 (2018) 383–389.
[33] D. Chen, Y. Wu, Z. Huang, J. Chen, Nano Micro Lett. 14 (2022) 156.
[34] L. Liu, J. Liu, K. Sun, et al., Chem. Eng. J. 411 (2021) 128629.
[35] D. Roy, K. Panigrahi, B.K. Das, et al., Nanoscale Adv. 3 (2021) 4739–4749.
[36] X. Chen, P. Ye, H. Wang, et al., Adv. Funct. Mater. 33 (2023) 2212915.
[37] Y. Yang, Y. Huang, S. Zhou, et al., J. Energy Chem. 72 (2022) 395–404.
[38] C. Wang, L.L. Gu, S.Y. Qiu, et al., Appl. Catal. B: Environ. 297 (2021) 120452.
[39] K. Zeng, W. Li, Y. Zhou, et al., Chem. Eng. J. 421 (2021) 127831.
[40] K. Xiang, D. Wu, Y. Fan, et al., Chem. Eng. J. 425 (2021) 130583.
[41] X. Qiao, H. Kang, Y. Li, et al., Appl. Catal. B: Environ. 305 (2022) 121034.
[42] M. Asnavandi, Y. Yin, Y. Li, C. Sun, C. Zhao, ACS Energy Lett. 3 (2018) 1515–1520.
[43] K. Zhang, G. Zhang, J. Qu, H. Liu, Small 14 (2018) 1802760.
[44] X. Wang, C. Sun, F. He, et al., ACS Appl. Mater. Interfaces 11 (2019) 32460–32468.
[45] S.J. Sitler, K.S. Raja, I. Charit, J. Electrochem. Soc. 163 (2016) H1069–H1075.
[46] W. Li, Y. Li, H. Fu, et al., Chem. Eng. J. 381 (2020) 122683.
[47] M. Zhang, Y. Liu, H. Zhao, et al., ACS Appl. Mater. Interfaces 13 (2021) 19904–19914.
[48] X. Hu, J. Wang, J. Wang, et al., Appl. Catal. B: Environ. 318 (2022) 121879.
[49] T. Zhao, D. Zhong, G. Hao, Q. Zhao, Appl. Surf. Sci. 607 (2023) 155079.
[50] Ö. Şahin, D.E. Karakaş, M. Kaya, C. Saka, J. Energy Inst. 90 (2017) 466–475.
[51] P. Li, Y. Huang, Q. Huang, et al., Appl. Catal. B: Environ. 313 (2022) 121444.
[52] J. Li, X. Hong, Y. Wang, et al., Energy Storage Mater. 27 (2020) 187–197.
[53] A. Tang, C. Wan, X. Hu, X. Ju, Nano Res. 14 (2021) 4063–4072.
[54] Y. Huang, L. Zhang, L.W. Jiang, et al., Small 19 (2023) 2302970.
[55] S. Zhou, L. Cheng, Y. Huang, et al., Appl. Catal. B: Environ. 328 (2023) 122519.
[56] H. Li, Z. Liu, L. Wang, et al., Chem. Eur. J. 29 (2023) e202203207.
[57] F.O. Baydaroglu, E. Özdemir, A.G. Gürek, Int. J. Hydrog. Energy 47 (2022) 9643–9652.
[58] H. Zhang, L. Zhang, I.A. Rodríguez-Pérez, et al., Appl. Surf. Sci. 540 (2021) 148296.
[59] P. Li, R. Chen, S. Zhao, et al., Appl. Catal. B: Environ. 298 (2021) 120523.
[60] H. Zhang, Y. Liu, H. Wei, et al., Appl. Catal. B: Environ. 314 (2022) 121495.
[61] S. Zhou, Y. Yang, W. Zhang, et al., J. Colloid Interface Sci. 591 (2021) 221–228.
[62] H. Wu, Y. Cheng, B. Wang, et al., J. Energy Chem. 57 (2021) 198–205.
[63] A. Sermiagin, D. Meyerstein, G.S. Rolly, et al., Int. J. Hydrog. Energy 47 (2022) 3972–3979.
[64] U.B. Demirci, P. Miele, C.R. Chim 17 (2014) 707–716.